

A multifrequency method based on the Matched Multifilter for the detections of point sources in CMB maps

L. F. Lanz^{1,2*}, D. Herranz¹, J. L. Sanz¹, J. González-Nuevo³ and M. López-Caniego^{1,4}

¹ *Instituto de Física de Cantabria, CSIC-UC, Av. de Los Castros s/n, Santander, 39005, Spain*

² *Departamento de Física Moderna, Universidad de Cantabria, Av. de Los Castros s/n, Santander, 39005, Spain*

³ *SISSA, via Beirut 4, I-34014 Trieste, Italy*

⁴ *Astrophysics Group, Cavendish Laboratory, J.J. Thomson Avenue, CB9 0E1, Cambridge, United Kingdom*

Received –, Accepted –

ABSTRACT

In this work we deal with the problem of simultaneous multifrequency detection of extragalactic point sources in maps of the Cosmic Microwave Background. We apply a linear filtering technique that uses spatial information and the cross-power spectrum. To make this, we simulate realistic and non-realistic flat patches of the sky at two frequencies of *Planck*: 44 and 100 GHz. We filter to detect and estimate the point sources and compare this technique with the monofrequency matched filter in terms of completeness, reliability, flux and spectral index accuracy. The multifrequency method outperforms the matched filter at the two frequencies and in all the studied cases in the work.

Key words: methods: data analysis – techniques: image processing – radio continuum: galaxies – cosmic microwave background – surveys

1 INTRODUCTION

Over the last few years, a big effort has been devoted to the problem of detecting point sources in Cosmic Microwave Background (CMB) experiments. The main reason is that modern CMB experiments have reached resolution and sensitivity levels such that their capability to estimate the statistics of CMB fluctuations at high multipoles is no longer limited by instrumental noise but by Galactic and extragalactic foreground contamination. Among extragalactic contaminants, point sources are the most relevant, both in temperature (Toffolatti et al. 1998; De Zotti et al. 1999; Hobson et al. 1999; De Zotti et al. 2005) and in polarisation (Tucci et al. 2004, 2005; López-Caniego et al. 2009). Moreover, they are one of the most difficult contaminants to deal with and, at least in the frequency range spanned by CMB experiments, one of the most poorly known. It is therefore mandatory to detect the maximum possible number of extragalactic point sources (EPS) and to estimate their flux with the lowest possible error before any serious attempt to study the CMB anisotropies.

But EPS are not only a contaminant to get rid of. The study of EPS at microwave frequencies is very interesting from the standpoint of extragalactic astronomy. The next generation of CMB experiments will allow one to obtain of

all-sky EPS catalogues that will fill in the existing observational gap in our knowledge of the Universe in the frequency range from 20 to roughly 1000 GHz. We expect to derive source number counts and spectral indices, to study source variability and to discover rare objects such as inverted spectrum radio sources, extreme gigahertz peaked spectrum sources (GPS) and high-redshift dusty proto-spheroids (see for example the *Planck Bluebook*, The Planck Collaboration 2006). The first fruits of these new era of CMB experiments are already here: the *Wilkinson Microwave Anisotropy Probe* (WMAP) satellite (Bennett et al. 2003) has made possible the obtaining of the first all-sky point source catalogues above ~ 0.8 –1 Jy in the 23–94 GHz range of frequencies in temperature (Bennett et al. (2003); Hinshaw et al. (2007); Chen & Wright (2008); Wright et al. (2009); López-Caniego et al. (2007); Massardi et al. (2009) and polarisation (López-Caniego et al. 2009), being complete the last three ones. In a recent paper González-Nuevo et al. (2008) have shown how these catalogues can be used to study the statistics of point sources in that range of frequencies. The *Planck* mission (Tauber 2005) will allow us to extend these catalogues down to lower flux limits and up to 857 GHz.

We have mentioned that the detection and estimation of the flux of EPS are a difficult task. The main reason for this is that the many different types of EPS that are distributed in the sky form a very heterogeneous set of objects

* E-mail: lanz@ifca.unican.es

that do not have a common spectral behaviour. While other foreground contaminants follow a specific emission law that is approximately well known (or can be inferred from observations) and that varies relatively slow and continuously across the sky, each extragalactic point source has an emission law, that, in principle, can be totally different to any other and independent from them. From the point of view of statistical signal processing, the problem of detecting EPS is a case of sorely under-determined component separation problem where the number M of components is much larger than the number N of frequency channels.

Let us consider the case of another contaminant that is of relevance in CMB images and to which the EPS problem has some similarities: the Sunyaev-Zel'dovich (SZ) effect (Sunyaev & Zeldovich 1970, 1972; Carlstrom et al. 2002). As in the case of EPS, the SZ contamination occurs in small and compact regions of the sky and it affects the high- ℓ region of the fluctuations angular power spectrum. But in the case of the thermal SZ effect the frequency dependence is very well known (ignoring relativistic corrections). This has made possible the development of a number of powerful detection techniques that are specifically suited to the problem of SZ effect detection in CMB images (Diego et al. 2002; Herranz et al. 002a; Hobson & McLachlan 2003; Pierpaoli et al. 2005; Herranz et al. 2005; Vale & White 2006; Pires et al. 2006; Melin et al. 2006; Bartlett et al. 2008; Leach et al. 2008) or to use more generic diffuse component separation techniques (see for example, among many others, Maino et al. 2002; Stolyarov et al. 2002; Delabrouille et al. 2003; Eriksen et al. 2004; Bedini et al. 2005; Bonaldi et al. 2006) to obtain SZ maps and catalogues.

Unfortunately, these approaches are not directly applicable to EPS detection. The most commonly used approach to this problem consists on working separately in each channel. The key idea is to take advantage of the fact that all the EPS have the same shape (basically, that of the beam). In the field of CMB images, wavelet techniques (Vielva et al. 2001, 2003; González-Nuevo et al. 2006; Sanz et al. 2006; López-Caniego et al. 2007), matched filters (MF, Tegmark & de Oliveira-Costa 1998; Barreiro et al. 2003; López-Caniego et al. 2006) and other related linear filtering techniques (Sanz et al. 2001; Chiang et al. 2002; Herranz et al. 002c; López-Caniego et al. 2004, 2005; López-Caniego et al. 2005) have proved to be useful. All these techniques rely on the prior knowledge that the sources have a distinctive spatial behaviour and this fact is used to design some bandpass filter to enhance them with respect to the noise. Detection can be further improved by including prior information about the sources, i.e. some knowledge about their flux distribution, in the frame of a Bayesian formalism (Hobson & McLachlan 2003; Carvalho et al. 2009).

With the previous single frequency methods and for the case of the *Planck* mission we expect to reach detection limit fluxes that range from a few hundred mJy to several Jy, depending on the frequency channel, and to obtain catalogues that will contain from several hundreds to a few thousand objects (López-Caniego et al. 2006; Leach et al. 2008). This is satisfactory, but we feel that we could do better if we were able to use multi-wavelength information in some way.

For now, multi-wavelength detection of EPS in

CMB images remains a largely unexplored field. In recent years, some attempts have been done in this direction (Naselsky et al. 2002; Chen & Wright 2008; Wright et al. 2009). More recently, Herranz & Sanz (2008) have introduced the technique of ‘*matched matrix filters*’ (MTXF) as the first fully multi-frequency, non-parametric, linear filtering technique that is able to find EPS and to do unbiased estimations of their fluxes thanks to the distinctive spatial behaviour of the sources, while at the same time does incorporate some multi-wavelength information, without assuming any specific spectral behaviour for the sources. Herranz et al. (2009) have applied the MTXF to realistic simulations of the *Planck* radio channels, showing that it is possible to practically double the number of detections, for a fixed reliability level, for some of the channels with respect to the single frequency matched filter approach.

MTXF use multi-wavelength information in such a way that it is not necessary to make any assumption about the spectral behaviour of the sources. In fact, in that formalism their spectral behaviour is entirely irrelevant. All the multi-wavelength considerations concern only to the noise¹ and its correlations. In this sense, MTXF deal only with half of the problem. This has its advantages in terms of robustness and reliability, but one could wish to have a technique that uses multi-wavelength information in the modelling of *both* the signal (EPS) and the noise. But, as we mentioned before, the spectral behaviour of the EPS is not known.

In this paper we will show that even if the spectral behaviour of the EPS is unknown a priori, it is still possible to determine it directly from the data by means of an adaptive filtering scheme that incorporates multi-frequency information not only through the noise correlations among channels, but also about the sources themselves.

The problem is, in more than one sense, similar to the problem of detecting SZ clusters (that is the reason we discussed that case a few paragraphs above). In the SZ case the spectral behaviour of the sources is known, but not their size. A way to deal with this is to introduce the scale of the source as a free parameter (for example, the cluster core radius r_c) in the design of a ‘*matched multifilter*’ (MMF) and to optimise the value of this parameter for each source so that a maximum signal to noise ratio is obtained after filtering (see the details in Herranz et al. 002a,b, 2005; Schäfer et al. 2006; Melin et al. 2006). As the problem depends on the optimisation of one single parameter, the method is easy to implement in codes that are relatively fast.

In this paper we introduce a modification of the MMF technique in which the mixing coefficients of the frequency dependence vector of the sources are considered as free parameters to be optimised. As we will show, if the number of frequency channels is N and we choose wisely a fiducial frequency of reference, the number of free parameters to optimise is $N - 1$. For simplicity, throughout this paper we will use as an example the case of two channels, $N = 2$, but the method is valid for any number of channels $N > 1$.

The structure of this paper is as follows. In section 2 we will summarise the formulae of the MMF and we will intro-

¹ Here the term ‘noise’ refers to all the components except for the EPS themselves, including CMB and Galactic foregrounds.

duce the modification that allows us to use it for detecting EPS in arbitrarily chosen pairs of frequency channels. We will show that the filter can be in this case factorised in such a way that a particularly fast implementation of the method can be achieved. In section 3 we will describe the simulations that we use to test the method. The results of the exercise will be described in section 4. Finally, in section 5 we will draw some conclusions.

2 METHOD

2.1 The single frequency approach

Let us assume a set of images corresponding to the same area of the sky observed simultaneously at N different frequencies:

$$y_\nu(\mathbf{x}) = f_\nu s_\nu(\mathbf{x}) + n_\nu(\mathbf{x}), \quad (1)$$

where $\nu = 1, \dots, N$. At each frequency ν , y_ν is the total signal in the pixel \mathbf{x} and s_ν represents the contribution of the point source to the total signal y_ν ; for simplicity let us assume there is only one point source centered at the origin of the image; f_ν is the frequency dependence of the point source; and n_ν is the *background* or generalized noise (containing not only the instrumental noise, but also the contributions of the rest of components).

The intrinsic angular size of the point sources is smaller than the angular resolution of the detector. At each observing frequency, each source is convolved with the corresponding antenna beam. For simplicity we will assume the antenna beam can be well described by a symmetric 2D Gaussian function. Then we can write

$$s_\nu(x) = A\tau_\nu(x), \quad (2)$$

where $x = |\mathbf{x}|$ (since we are considering symmetric beams), A is the *amplitude* of the source and τ is the spatial template or *profile*. The background $n_\nu(\mathbf{x})$ is modelled as a homogeneous and isotropic random field with average value equal to zero and power spectrum P_ν defined by

$$\langle n_\nu(\mathbf{q})n_\nu^*(\mathbf{q}') \rangle = P_\nu \delta_D^2(\mathbf{q} - \mathbf{q}'), \quad (3)$$

where $n_\nu(\mathbf{q})$ is the Fourier transform of $n_\nu(\mathbf{x})$ and δ_D^2 is the 2D Dirac distribution.

In the single frequency approach each channel is processed separately and independently from the other frequency channels. This approach is robust in the sense that it is not necessary to assume anything about the spectral behaviour of the sources. The main drawback of the single frequency approach, however, is that one misses the potential noise reduction that could be obtained with a wise use of the information present at the other frequencies.

The standard single frequency point source detection method in the literature is based on the *matched filter* (Tegmark & de Oliveira-Costa 1998; Barreiro et al. 2003; López-Cañiego et al. 2006). The matched filter is the optimal linear detector for a single map in the sense that it gives the maximum signal to noise amplification. The matched filter can be expressed in Fourier space in the following way:

$$\psi_{MF}(q) = \frac{\tau(q)}{aP(q)}, \quad a = \int d\mathbf{q} \frac{\tau^2(q)}{P(q)}. \quad (4)$$

Here a is a normalisation factor that preserves the source amplitude after filtering.

2.2 The Matched Multifilter

In the multi-frequency approach we take into account the statistical correlation of the noise between different frequency channels and the frequency dependence of the sources. Now let us model the background $n_\nu(\mathbf{x})$ as a homogeneous and isotropic random field with average value equal to zero and crosspower spectrum $P_{\nu_1\nu_2}$ defined by:

$$\langle n_{\nu_1}(\mathbf{q})n_{\nu_2}^*(\mathbf{q}') \rangle = P_{\nu_1\nu_2} \delta_D^2(\mathbf{q} - \mathbf{q}') \quad (5)$$

where $n_\nu(\mathbf{q})$ is the Fourier transform of $n_\nu(\mathbf{x})$ and δ_D^2 is the 2D Dirac distribution. Let us define a set of N linear filters ψ_ν that are applied to the data

$$w_\nu(\mathbf{b}) = \int d\mathbf{x} y_\nu(\mathbf{x})\psi_\nu(\mathbf{x}; \mathbf{b}) = \int d\mathbf{q} e^{-i\mathbf{q}\cdot\mathbf{b}} y_\nu(\mathbf{q})\psi_\nu(q). \quad (6)$$

Here \mathbf{b} defines a translation. The right part of equation (6) shows the filtering in Fourier space, where $y_\nu(\mathbf{q})$ and $\psi_\nu(q)$ are the Fourier transforms of $y_\nu(\mathbf{x})$ and $\psi_\nu(\mathbf{x})$, respectively. The quantity $w_\nu(\mathbf{b})$ is the filtered map ν at the position \mathbf{b} . The *total filtered map* is the sum

$$w(\mathbf{b}) = \sum_\nu w_\nu(\mathbf{b}). \quad (7)$$

Therefore, the total filtered field is the result of two steps: a) filtering and b) fusion. During the first step each map y_ν is filtered with a linear filter ψ_ν ; during the second step the resulting filtered maps w_ν are combined so that the signal s is boosted while the noise tends to cancel out. Note that the fusion in eq. (7) is completely general, since any summation coefficients different than one can be absorbed in the definition of the filters ψ_ν . Then the problem consists in how to find the filters ψ_ν so that the total filtered field is *optimal* for the detection of point sources.

The total filtered field w is *optimal* for the detection of the sources if

- (i) $w(\mathbf{0})$ is an *unbiased* estimator of the amplitude of the source, so $\langle w(\mathbf{0}) \rangle = A$;
- (ii) the variance of $w(\mathbf{b})$ is minimum, that is, it is an *efficient* estimator of the amplitude of the source.

If the profiles τ_ν and the frequency dependence f_ν are known and if the crosspower spectrum is known or can be estimated from the data, the solution to the problem is already known: the matched multifilter (MMF, Herranz et al. 002a):

$$\Psi(q) = \alpha \mathbf{P}^{-1}\mathbf{F}, \quad \alpha^{-1} = \int d\mathbf{q} \mathbf{F}^t \mathbf{P}^{-1}\mathbf{F}, \quad (8)$$

where $\Psi(q)$ is the column vector $\Psi(q) = [\psi_\nu(q)]$, \mathbf{F} is the column vector $\mathbf{F} = [f_\nu\tau_\nu]$ and \mathbf{P}^{-1} is the inverse matrix of the cross-power spectrum \mathbf{P} . Finally, we can obtain the variance of the total filtered field, given by the following expression:

$$\sigma_w^2 = \int d\mathbf{q} \Psi^t \mathbf{P} \Psi = \alpha \quad (9)$$

2.3 MMF with unknown source frequency dependence

As it was previously discussed, the problem is that the frequency dependence f_ν of the sources is not known a priori. Then, the possibilities are either a) to admit defeat, returning to the single frequency approach, b) to devise a filtering method that does not use the frequency dependence of the sources altogether or c) to model somehow the unknown frequency dependence in the framework of some optimisation scheme. The second approach was explored in Herranz & Sanz (2008); Herranz et al. (2009). In this work we will study the third approach to the problem.

Before addressing this problem, it will be useful to rewrite eq.(8) in a slightly different way. Let us write the vector $\mathbf{F} = [f_\nu \tau_\nu]$ in matrix form as

$$\mathbf{F} = \mathbf{T}(q)\mathbf{f}(\nu), \quad (10)$$

with \mathbf{T} a diagonal matrix $\mathbf{T}(q) = \text{diag}[\tau_1(q), \dots, \tau_N(q)]$ and $\mathbf{f} = [f_\nu]$ the vector of frequency dependences. Note that all the dependence in q is included in the matrix \mathbf{T} ; this fact will be useful later.

Now imagine that \mathbf{f} describes the true (unknown) frequency dependence of the sources and that $\mathbf{g} = [g_\nu]$, $\nu = 1, \dots, N$ is a new vector, of equal size as \mathbf{f} but whose elements can take any possible value. We can define the MMF for vector \mathbf{g}

$$\begin{aligned} \Psi_{\mathbf{g}}(q) &= \alpha_{\mathbf{g}} \mathbf{P}^{-1} \mathbf{T} \mathbf{g}, \\ \alpha_{\mathbf{g}}^{-1} &= \int d\mathbf{q} \mathbf{g}^t \mathbf{T} \mathbf{P}^{-1} \mathbf{T} \mathbf{g} = \mathbf{g}^t \mathbf{H} \mathbf{g}, \end{aligned} \quad (11)$$

where $\mathbf{H} = \int d\mathbf{q} \mathbf{T} \mathbf{P}^{-1} \mathbf{T}$ and we have used the facts that $\mathbf{T}^t = \mathbf{T}$ and that vector \mathbf{g} does not depend on \mathbf{q} and can therefore go out of the integral. When applied to a set of images where there is present a point source with true amplitude A and true frequency dependence \mathbf{f} , the filters $\Psi_{\mathbf{g}}$ will lead to an estimation of the amplitude

$$A_{\mathbf{g}} = w_{\mathbf{g}}(\mathbf{0}) = \alpha_{\mathbf{g}} A \mathbf{g}^t \mathbf{H} \mathbf{f}. \quad (12)$$

Note that if $\mathbf{g} \neq \mathbf{f}$, then $A_{\mathbf{g}} \neq A$. On the other hand, the variance of the filtered field would be, in analogy with eq. (9), $\sigma_{\mathbf{g}}^2 = \alpha_{\mathbf{g}}$. Let us finally define the signal to noise ratio of the source in the total filtered map as

$$SNR_{\mathbf{g}} = \frac{A_{\mathbf{g}}}{\sigma_{\mathbf{g}}}. \quad (13)$$

Then we can ask what is the vector \mathbf{g} that maximizes the signal to noise ratio $SNR_{\mathbf{g}}$. Intuition alone indicates that $SNR_{\mathbf{g}}$ is maximum if and only if $\mathbf{g} = \mathbf{f}$. This can be formally proved with little effort by taking variations of \mathbf{g} .

Then the problem can be solved via a maximisation algorithm. In the case of a non blind search, where the position of a given point source is known, one can focus on that point source and iteratively try values of the elements of \mathbf{g} until a maximum signal to noise is reached. In the case of a blind search, the situation is a little bit more difficult because in a given image there may be many different objects s_i with a different solution \mathbf{g}_i . A way to proceed is to filter many times the image, using each time a different set of values of the elements of \mathbf{g} so that the appropriate range of frequency dependences is sufficiently well sampled, and then to proceed counting one by one all the possible detections

and associating to each one the values of \mathbf{g} that maximize the signal to noise ratio of that source in particular.

We would like to remark that this situation is very similar to the case of the detection of galaxy clusters with unknown angular size described in Herranz et al. (002a,b). In that case the frequency dependence \mathbf{f} was known but the size of the clusters (their source profile) was not. The cluster profile can be parametrised as a modified beta profile with a free scale parameter r_c (typically, the cluster core radius). In Herranz et al. (002a,b) it was shown that the true scale of the clusters can be determined by maximizing the signal to noise ratio of the detected clusters as a function scale r_c of the filter.

In our case, factorisation (10) leads to equations (11) and (12); this is very convenient for implementation of the MMF when many filtering steps are necessary. The most time-consuming part of the filter is the calculation of matrices \mathbf{P} and \mathbf{T} because they must be calculated for all values of \mathbf{q} . In the case of clusters with unknown size \mathbf{T} had to be calculated for every value of r_c . However, in the case we are considering in this paper the only quantity that varies during the maximisation process are the elements of vector \mathbf{g} . This allows us to compute the integrals of matrix \mathbf{H} only once for each set of images. As a result, applying the MMF to large numbers of point sources with unknown frequency dependence is, in general, much faster than applying the MMF to the same number of clusters with unknown source profile.

The main difference is that while in the case of galaxy clusters it was necessary to maximize with respect to only one single parameter (the core radius), in the case of the unknown frequency dependence it is necessary to maximize with respect to the N components of vector \mathbf{g} . This procedure can require a very large number of computations if N is big. Although we have just seen that each free parameter of the frequency dependence can be mapped much faster than each free parameter of the source profile, we are still interested in reducing the number of computations as much as possible.

2.4 Number of degrees of freedom of vector \mathbf{g}

For N images, vector $\mathbf{g} = [g_1, \dots, g_N]$ has N degrees of freedom. This makes the optimisation procedure more complex and computationally expensive. The situation can be lightened if we choose one of the frequencies under consideration as our fiducial frequency of reference. Let us choose for example a concrete frequency $j \in \{1, \dots, N\}$ to be our fiducial frequency of reference, then

$$\langle y_j(0) \rangle = A f_j \tau_j(0) = A \quad (14)$$

and therefore, since the profile τ_j is normalised to unity, f_j must be equal to one. Therefore, we must look for vectors $\mathbf{g} = g_1, \dots, g_{j-1}, 1, g_{j+1}, \dots, N$ and the number of independent degrees of freedom is $N - 1$. If the number of channels is $N = 2$, there is only one degree of freedom for the optimisation problem. In the next sections of this paper we will consider, for simplicity, the case of two channels, but we would like to remark that the extension to $N > 2$ frequencies is straightforward.

2.5 Optional parametrisation of vector \mathbf{g}

Another way to reduce the number of degrees of freedom of vector \mathbf{g} is to find a suitable parametrisation for it. For example, the power law relationship

$$I(\nu) = I_0 \left(\frac{\nu}{\nu_0} \right)^{-\gamma}, \quad (15)$$

where $I(\nu)$ is the flux at frequency ν , ν_0 is a frequency of reference, I_0 is the flux at that frequency of reference and γ is the *spectral index*, is widely used in the literature. If eq. (15), then the reference flux I_0 can easily be related to the reference amplitude A of the sources and the number of degrees of freedom is just one, the spectral index γ .

However, the parametrisation of vector \mathbf{g} has its own risks. For example, it is known that eq. (15) is valid only as an approximation for any given frequency interval and that its validity decreases as the size of the interval grows. If we choose to follow the parametric approach we know for sure that the results will be less and less accurate as the number N of channels grows, especially if the separation between frequency channels is large. On the other hand, eq. (15) is always exact if $N = 2$. Therefore we can safely use the parametrisation (15) for $N = 2$ channels, without loss of generality. Since the number of degrees of freedom is one either if (15) is used or not, the use of the parametrisation is irrelevant in this case. However, we may be interested in using it for historical, didactic and practical motivations. For example, eq. (15) is useful to express the physical properties of the sources in terms of their (steep, flat, inverted, etc.) spectral index.

We would like to remark that frequency dependence parametrisation, in the form of eq. (15) or any else other way, may or not be useful in some cases, but *it is not essential* at all for the method we propose in this paper.

3 SIMULATIONS

In order to illustrate the MMF method described above and to compare the MMF multi-frequency approach with the single frequency approach, we have performed a set of basic, yet realistic, simulations. We consider the case of two frequency channels ($N = 2$). Generalisation to more frequency channels is possible, as discussed in section 2.3, but we choose to keep things simple in this paper.

For this example we take the case of the *Planck* mission (Tauber 2005). We will consider the 44 GHz and 100 GHz *Planck* channels. The choice of the pair channels is not essential: any other pair of channels would have served the same for this exercise. This particular choice allows to study the case of radio sources in two not adjoining channels with different instrumental settings: the 44 GHz channel belongs to the Low Frequency Instrument of *Planck* and the 100 GHz channel belongs to the High Frequency Instrument.

For the simulations we have used the *Planck* Sky Model² (PSM, Delabrouille et al. 2009, in preparation), a flexible software package developed by *Planck* WG2 for

making predictions, simulations and constrained realisations of the microwave sky. The simulated data used here are the same as in Leach et al. (2008), where the characteristics of the simulations are explained in more detail. Maps are expressed in $(\Delta T/T)$, thermodynamic units. Simulations include all the relevant astrophysical components: the CMB sky is based on a Gaussian realisation assuming the WMAP best-fit C_ℓ at higher multipoles; Galactic emission is described by a three component model of the interstellar medium comprising free-free, synchrotron and dust emissions. Free-free emission is based on the model of Dickinson et al. (2003) assuming an electronic temperature of 7000 K. The spatial structure of the emission is estimated using a H α template corrected for dust extinction. Synchrotron emission is based on an extrapolation of the 408 MHz map of Haslam et al. (1982) from which an estimate of the free-free emission was removed. A limitation of this approach is that this synchrotron model also contains any dust anomalous emission seen by WMAP at 23 GHz. The thermal emission from interstellar dust is estimated using model 7 of Finkbeiner et al. (1999).

For the purely descriptive purposes of this example, we take eight different regions of the sky located at intermediate Galactic latitude (four of them uniformly distributed across the 40° North Galactic latitude parallel and four of them distributed in the same way 40° South of the Galactic plane). For each region we select a 512×512 pixel square patch (at 44 and 100 GHz). Pixel size is 1.72 arcmin for the two frequencies. Therefore, each patch covers an area of 14.656 square degrees of the sky. When both patches have been selected, we add simulated extragalactic point sources with a spectral behaviour described by eq. (15). We take as frequency of reference $\nu_0 = 44$ GHz. Note that eq. (15) is expressed in flux units and the maps are in $(\Delta T/T)_{th}$: we make the appropriate unit conversion before adding the sources. The antenna beam is also taken into account: the full width at half maximum is FWHM=24 arcmin for the 44 GHz channel and FWHM=9.5 arcmin at 100 GHz. Finally, after doing that, we have added to each patch uniform white noise with the nominal levels specified for *Planck* (The Planck Collaboration 2006) and this pixel size.

We are interested in comparing the performance of the multi-frequency approach with that of the single-frequency matched filter. In particular, we expect to be able to detect fainter sources with the MMF than with the MF. From recent works (López-Caniego et al. 2006; Leach et al. 2008) we know that in this kind of *Planck* simulations, the MF can detect sources down to fluxes ~ 0.3 Jy (the particular value depends on the channel and the region of the sky). Here we will simulate sources in the interval $[0.1, 1.0]$ Jy plus a few cases, that will be described below, where even lower fluxes are necessary. Regarding the spectral index of the sources, according to González-Nuevo et al. (2008), most radio galaxies observed by WMAP at fluxes ~ 1 Jy show spectral indices that lie in the range $(-1.0, 1.4)$.

We sample the interesting intervals of flux and spectral index by simulating sources with fluxes at 44 GHz $I_0 = \{0.1, 0.2, 0.3, 0.4, 0.5, 0.6, 0.7, 0.8, 0.9, 1.0\}$ Jy and spectral indices $\gamma = \{-1.0, -0.7, -0.4, -0.1, 0.2, 0.5, 0.8, 1.1, 1.4\}$. For each pair of values (I_0, γ) we have simulated 100 point sources. The point sources are randomly distributed in the

² http://www.apc.univ-paris7.fr/APC_CS/Recherche/Adamis/PSM/psky-en.php

maps (obviously, the same source is placed in the same pixel in both frequencies), with only one constraint: it is forbidden to place a source closer than $FWHM_{44}/2$ pixels from any other. In this way we avoid source overlapping. Image borders are also avoided. For each set of 100 sources we proceed in the following way: we randomly choose one among the eight patches we have and place 10 sources in it. Then we randomly choose other patch (allowing repetition) and place the next 10 sources, and so on. In total, we have simulated 9000 sources for this exercise (the additional simulations at fluxes below 0.1 Jy are not included).

4 RESULTS AND DISCUSSION

In order to compare the *matched filter* and the *matched multifilter*, we use the same maps with both methods. It means that not only the maps, but the sources are identical for the two filters (their intrinsic fluxes and positions). Each simulation is filtered separately with the matched filter (4) and the matched multifilter (8). In order to have a better estimation of the power spectra, avoiding as much as possible aliasing effects, we implement a power spectrum estimator that uses the 2D Hann window (Jiang et al. 2002).

We will compare performance of the two methods in terms of the following aspects: spectral index estimation, source detection and flux estimation.

4.1 Source detection

Direct comparison of source detection between the MF and the MMF is not an obvious task because for $N = 2$ input images the MF produces two filtered images, whereas the MMF produces only one combined filtered map. Whereas the meaning of ‘detection’ in the latter case is straightforward (once a detection criterion is chosen, a source is detected or not), in the former the situation is not so clear. Imagine we decide to apply the same detection criterion to the two MF filtered images (which is not an obvious option), then for a given source we can have three different outcomes of the detection:

- The source may be detected in both maps.
- The source may be detected in only one of the maps.
- The source may be detected in none of the maps.

In the first two cases we can obtain point source catalogues (with different number of objects, in principle, for the two frequencies), but only in the first case are we able to estimate the flux at the two frequencies and therefore the spectral index. In the case of the MMF, if the source is detected we automatically know the spectral index and we can use eq. (15) to give the fluxes at the two frequencies.

Therefore, in the following we will distinguish two different cases when we speak about detections with the MF. On the one hand, the *intersection* of the detections in the two channels gives us the objects that can be used for studying the spectral index distribution; on the other hand, the *union* of the two sets gives us the total number of objects that can be detected in, at least, one of the channels. For the MMF, both sets are the same by definition.

Regarding the detection criterion, for simplicity we will apply the same criterion to all the filtered maps: the

widespread 5σ threshold. Note that the 5σ threshold corresponds to different flux values for different filters. However, in this paper we will follow the standard 5σ criterion for simplicity.

Figure 1 shows the real sources (in %) that we detect above a 5σ level detection whose intrinsic fluxes (values introduced by us in the simulations) in the reference frequency (I_0) are the corresponding values in the horizontal axis. Table 1 shows the flux at which we are able to detect, at least, the 95% of the sources. We can observe several interesting aspects. The first one is the fact that the matched multifilter improves the level of detection with respect to the matched filter level for all the values of γ we have inserted.

The second one is a natural selection effect: we detect more flat/inverted sources ($\gamma \sim 0$ / negative values of γ) at low fluxes than steep ones (positive values of γ). Figure 1 and Table 1 show us that the level of detections is higher for negative values of γ than for positive values. Keeping in mind that the reference frequency ν_0 is equal to 44 GHz, and according to eq. (15), it can be seen that for $\gamma > 0$, the simulated sources satisfy this condition: $I_{100} < I_{44}$. In this case, the sources appear less bright at 100 GHz. In these conditions it is quite difficult to detect sources at 100 GHz. Therefore, it means that we are not able to give the spectral indices of these point sources by means of the matched filter method when γ is strongly positive (for instance, $\gamma \gtrsim 1$). Obviously, the smaller γ is, the better the detection is with the matched filter at 100 GHz. Therefore, we add from $\gamma = -0.1$ two additional bins at $I_0 = 25, 50$ mJy.

Another aspect we have to remark is the similar aspect of the detection curve for the matched filter at 44 GHz for all the γ values (see Figure 1). The reason of this similarity is that the reference frequency is 44 GHz, and the maps we have simulated at this frequency are the same, independently of γ , with only one exception: the position of the sources. This means that statistically are equivalent (with the inherent fluctuations due to the variation in the positions of the sources). We find a similar number of detections by means of the matched filter at 44 GHz, independently of γ . For this reason it is difficult to characterize the spectral behaviour of the sources for $I_0 \lesssim 0.5$ Jy, because we do not have a high percentage of detected sources at 44 GHz below that value of I_0 .

Additionally, we observe that the matched multifilter is capable to detect sources whose $I_0 < 0.1$ Jy for $\gamma \lesssim -0.1$. It is interesting to compare this with the matched filter, that does not detect sources below 0.1 Jy in the conditions of this work. This is a result that we obtain with the method presented here. It allows us to detect point sources whose I_0 is too low to be detected with the traditional matched filter.

To summarise, we can say that the MMF improves the detection level. Specially remarkable are the cases where the sources are near to be *flat* (central row of Figure 1). At 100 GHz, the MF recovers the 100% of the sources for $I_0 \sim 0.4 - 0.6$ Jy. Meanwhile, the MMF reaches this level for $I_0 \sim 0.1$ Jy. This particular case is really interesting in the sense that most of the sources have this spectral behaviour.

4.2 Spectral index estimation

As it was mentioned before, one of the quantities we want to obtain is the spectral index of the sources (eq. 15). As we

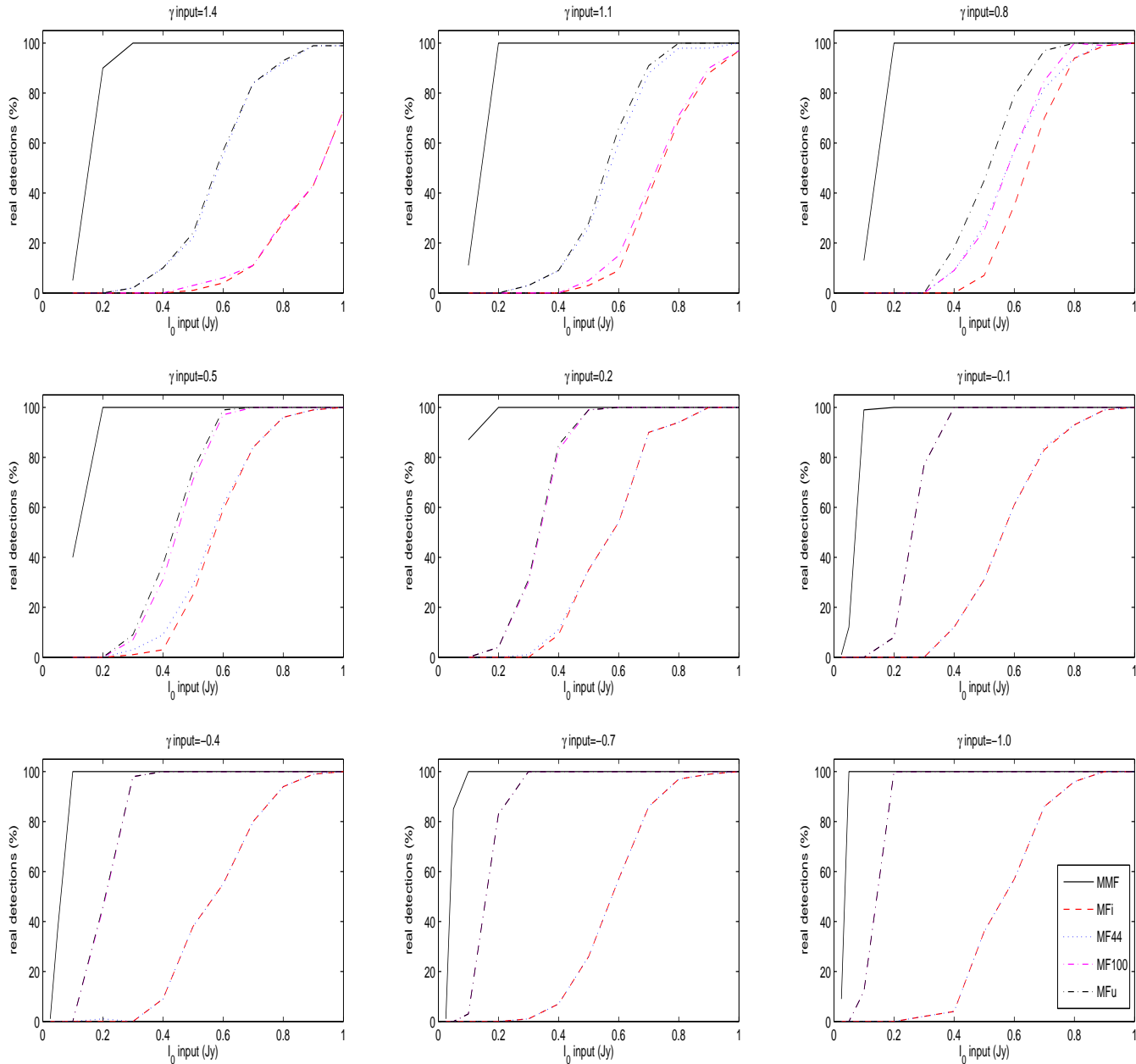


Figure 1. Number of detections against the input value of I_0 for different values of the spectral index γ . MF44 represents the sources detected with the matched filter at 44 GHz. MF100 the same but at 100 GHz. MF i is the intersection of MF44 and MF100, and MF u is the union of MF44 and MF100.

can see in that equation, when we know this spectral index and the flux at the reference frequency, we are able to give an estimation of the flux at other channels. In Figure 2 we see how we recover the spectral index by means of the MMF, and compare these results with the obtained by the matched filter. In general, we can observe that we can reach lower values of I_0 with the MMF. Also, at higher values of I_0 than

$\gtrsim 0.4$ Jy, we are able to give, with a good degree of precision, an estimation of γ by means of the multifrequency method. In general, the error bars at these values of I_0 are quite smaller than the bars of the matched filter, so we recover with more accuracy the spectral index and less uncertainty.

Other aspect is that the error bars increases when I_0 is smaller. It seems logical, because we have fainter sources

γ	$I_0(MMF)_{95\%}(Jy)$	$I_0(MF_{44})_{95\%}(Jy)$	$I_0(MF_{100})_{95\%}(Jy)$	$I_0(MFi)_{95\%}(Jy)$	$I_0(MFu)_{95\%}(Jy)$
1.4	0.3	0.9	>1.0	>1.0	0.9
1.1	0.2	0.8	1.0	1.0	0.8
0.8	0.2	0.9	1.0	0.9	0.7
0.5	0.2	0.8	0.6	0.8	0.6
0.2	0.2	0.9	0.5	0.9	0.5
-0.1	0.1	0.9	0.4	0.9	0.4
-0.4	0.1	0.9	0.3	0.9	0.3
-0.7	0.1	0.8	0.3	0.8	0.3
-1.0	0.05	0.8	0.2	0.8	0.2

Table 1. Fluxes in the reference frequency (I_0) for which we detect, at least, the 95% of the sources for the different filtering methods. MMF, MF44, MF100, MFi, MFu as the Figure 1.

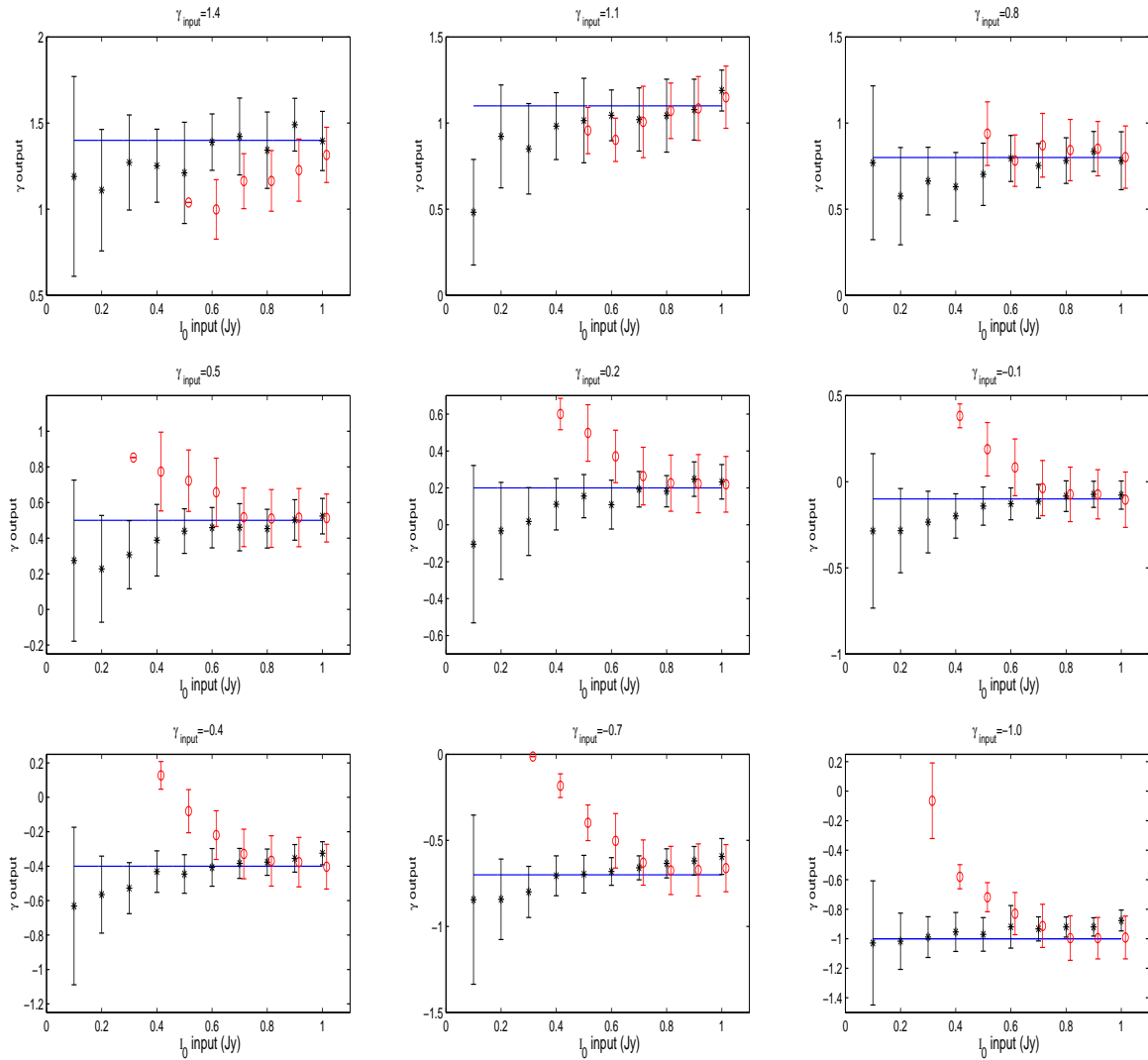


Figure 2. Values of γ recovered by means of the MMF (asterisks) and the MF (circles). The line indicates the ideal recovering. The circles corresponding to the MF are slightly displaced in the horizontal axis in order to distinguish the results.

and a smaller number of detections (see Figure 1). Then, at $I_0 = 0.1$ Jy, we can see that the estimation of γ is not as good as we wish, because it has a great uncertainty. The main reason is that the signal to noise ratio is close to the threshold level we have imposed.

With the matched filter we estimate correctly the spectral index for $I_0 \gtrsim 0.7$ Jy at $\gamma \leq 0.8$. At higher values of γ we find the same problem that we have mentioned before: there are not so many detections at 100 GHz below 0.7 Jy (Figure 1). Since the detected sources are close to the noise level, the fluxes recovered present an overestimation with respect to the input value due to the Eddington bias (Eddington 1913), an effect produced close to the noise level by the overestimation due to the fluctuations because of the noise in the positions where the source is located. As we said before, and seeing the Figure 1, we detect more sources at 100 GHz than at 44 GHz for values of the spectral index smaller than 0.8.

Finally, we can observe an interesting aspect of the matched filter. When we do not have the sufficient detections in, at least, one channel (the sources detected are below the $\sim 40\%$ of the total number of sources), the estimation of the spectral index is not good. In all cases we see an overestimation of γ , except for $\gamma = 1.4, 1.1$, where we have an underestimation. This is due to the fact that at these values of γ the sources at 100 GHz are fainter and the number of detections at this channel is really small. Then, because of the Eddington bias, the flux at this frequency is overestimated, and consequently, the value of γ is underestimated. The Eddington bias explains as well the overestimation of γ in the other cases. The only difference is that now, it is at 44 GHz where we have a smaller number of detections. If we also see the Figure 1, we observe that for values of $I_0 \lesssim 0.6$ Jy, we are pretty close to the noise level. It means that the noise fluctuations in the maps produce an overestimation in the flux at 44 GHz (I_0) and, in this case, an overestimation in γ too. Summarising, for $\gamma = 1.4, 1.1$, the Eddington bias appears at 100 GHz (underestimation of the spectral index). For the rest of values of γ , this bias appears at 44 GHz (overestimation of the spectral index).

4.3 Flux estimation

The other quantity that we want to recover is the flux of the source at the reference frequency ν_0 . As we said in section 4.2, and according to eq. 15, when we obtain the flux at ν_0 , we are able to estimate the flux at 100 GHz.

Figure 3 shows the recovered flux at the reference frequency (44 GHz) for a given value of the spectral index. The error bars recovered with the matched filter are, in general, larger than the ones we obtain with the matched multifilter. It is particularly notorious at small values of I_0 , where the recovered values of the flux have a good agreement with respect to the input values, with small error bars.

We observe in Figure 3 the evolution of the recovered flux. In general, for all the values of γ that we have studied, the matched multifilter is a suitable and effective tool to estimate the I_0 of the sources. For the matched filter, we observe a good determination of I_0 for input values above 0.7 Jy. For smaller values, I_0 has a higher value than its real one. That is due to the Eddington bias at 44 GHz. At this frequency, in Figure 1 we observe that for values smaller than

0.6 Jy, we only detect a $\sim 40\%$ of the total sources. That means that many of these sources are close to this noise level. And for the correct estimation of I_0 and the spectral index, we need a good detection of the sources at the two channels. For low values of I_0 the number of detected objects is small and we have few statistics.

In this section we have discussed about the flux at the reference frequency (44 GHz in our case). But we have used the matched multifilter with two different frequencies. For this reason it is necessary to say something related to the second channel at 100 GHz. It is important to obtain the values that we recover at 100 GHz with the matched multifilter because the corresponding errors bars of I_0 and γ could propagate additional errors in the flux estimation at 100 GHz (see eq. (15)). After extrapolating the results, we obtain the flux at 100 GHz, and compare it with the results obtained with the matched filter. As we saw at 44 GHz, the improvement with the matched multifilter is clear respect to the matched filter.

4.4 Reliability

For academic purposes, in the previous sections, we have produced the simulations introducing 100 sources for each of the pair values of intensity and spectral index (see section 3), that simplifies the comparison between both filters for all the cases under study. On the contrary, it is well known that the number of sources per flux interval, the source number counts, is not constant (De Zotti et al. 2005; González-Nuevo et al. 2008) nor the spectral index distribution (Sadler et al. 2008; González-Nuevo et al. 2008; Massardi et al. 2009). In order to study the performance of the new method under more realistic simulations we produced a new set of simulations (100) with the following characteristics:

- We used as a background the same eight regions described in the previous sections.
- The sources were simulated with an almost Poissonian distribution (see González-Nuevo et al. (2005) for more details about the method) at 44GHz, with fluxes that follow the source number counts model of De Zotti et al. (2005).
- The fluxes at 100GHz were estimated assuming random spectral indices from the González-Nuevo et al. (2008) distribution.
- The point source maps were filtered with the same resolution as the background maps and randomly added to them.

There is also another interesting quantity commonly used in the study of the performance of a source detector: the number of spurious sources. Spurious sources are fluctuations of the background that satisfied the criteria of the detection method and therefore are considered as a detected sources. It is clear that the best method will be the one that has the best detections vs. spurious ratio. Therefore, this time we use more realistic simulations and count the spurious and real sources: the maps are filtered using the MMF and the MF at both frequencies, we estimate the position and intensity of the sources above 3σ level and, by comparing with the input source simulations, we count the number of real and spurious sources that we are able to detect. It is necessary to change the detection level from 5σ to 3σ in order to observe spurious sources and make the following analysis.

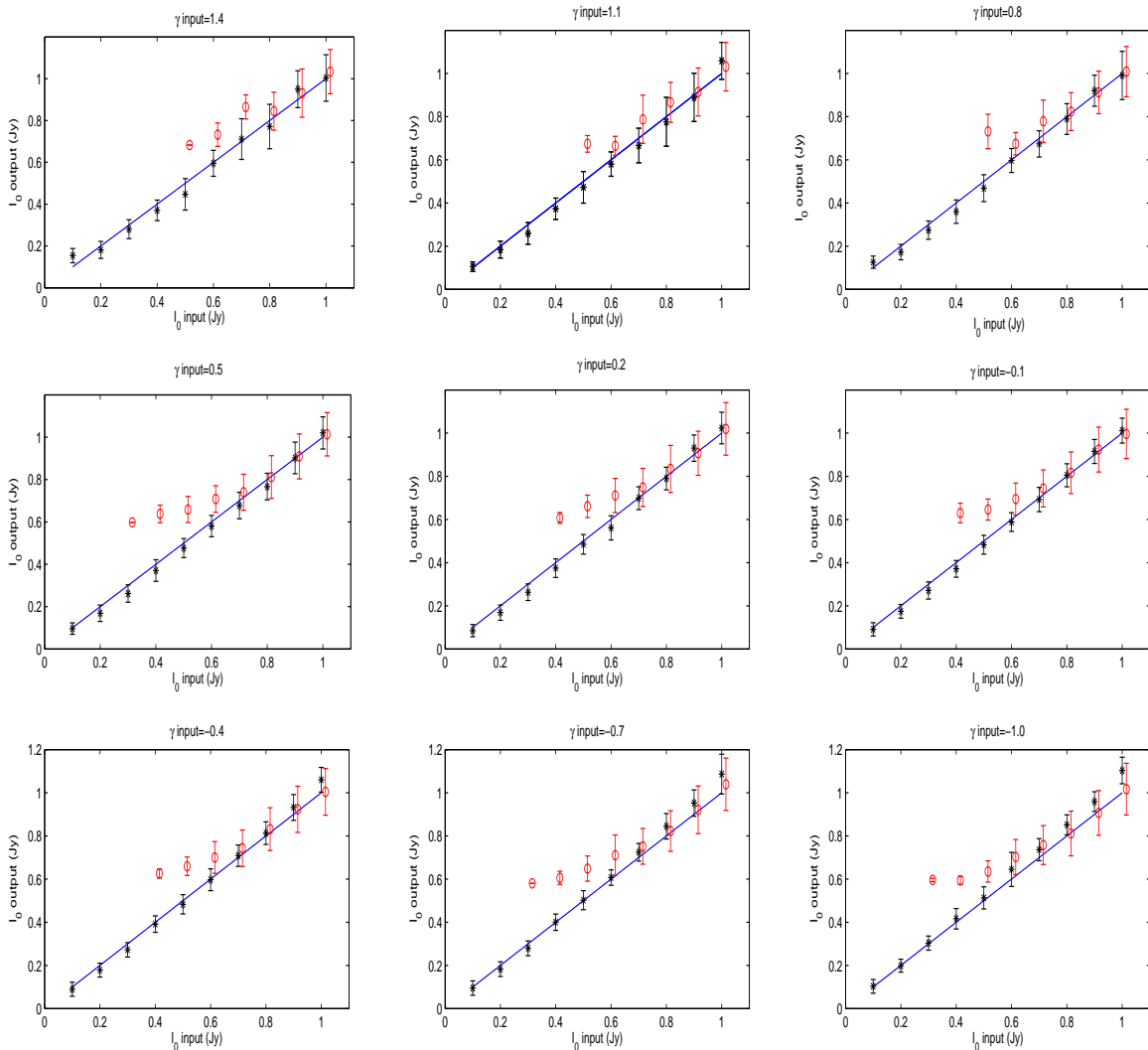


Figure 3. Values of I_0 (flux at 44 GHz) recovered by means of the MMF (asterisks) and the MF (circles). The line indicates the ideal recovering. The circles corresponding to the MF are slightly displaced in the horizontal axis in order to distinguish the results.

In Figure 4 we observe the number of real sources that both methods are capable to detect, whose intrinsic fluxes are higher than the corresponding value in the horizontal axis. As we can observe at 44 GHz, MMF detects a higher number of real sources for fluxes below $\sim 0.4 - 0.5$ Jy, being this difference very important at lower fluxes. Therefore, we obtain a clear improvement using the MMF with respect to the traditional matched filter at low fluxes. At 100 GHz, we observe a similar behaviour, but in this case the differences between the MF and the MMF start at ~ 0.2 Jy. If we observe the Figure 1, we notice that the number of sources detected with the MF is higher at 100 GHz than at 44 GHz for values of the spectral index between 0 and 0.5. These values of γ , according to the model used to simulate the point sources in this section, are the most frequent in the

real sources. This gives us an idea about why the detection level of the MF is higher at 100 GHz.

In Figure 5 we compare the *reliability* of both methods at 44 and 100 GHz. Reliability above a certain recovered flux is defined as $r = N_d / (N_d + N_s)$, where N_d is the number of real sources above that flux, and N_s is the number of spurious sources above the same flux. At 44 GHz we reach a $\sim 100\%$ of reliability at fluxes of ~ 0.3 Jy. However, the MF at this frequency reaches this level of reliability when the sources have fluxes of $\sim 0.9 - 1.2$ Jy. At 100 GHz we obtain better levels of reliability. For example, with the MMF we have at 0.1 Jy more than 95% of reliability, and the MF reaches these values for fluxes of ~ 0.3 Jy. According to the expression of the reliability, this number gives us the percentage of real sources over the total number of sources detected after filtering. Therefore, we can say that the MMF

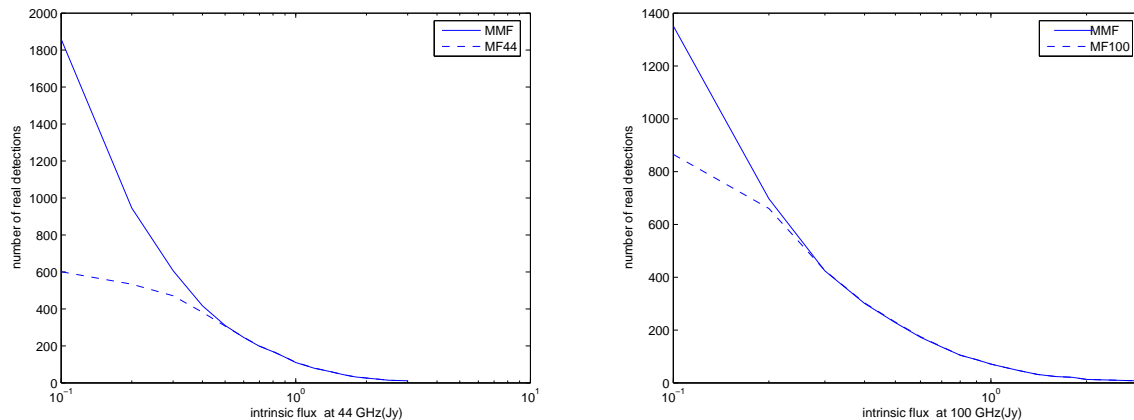


Figure 4. Number of real sources recovered by the MMF (solid line) and the MF (dashed line) at 44 GHz (left panel) and 100 GHz (right panel) whose intrinsic fluxes are higher than the corresponding value in the x axis.

is more reliable than the MF, specially at lower fluxes. Additionally, we can establish the flux for which we have the 5% of spurious sources. Making easy calculations, we finally obtain that the fluxes for which we have this percentage of spurious detections with the MF at 44 and 100 GHz are $\sim 0.5 - 0.6$ Jy and 0.25 Jy respectively. If we compare these values with the MMF, we obtain that the fluxes are 0.15 Jy and < 0.1 Jy. With these numbers one can see that the percentage of spurious detections of the MMF is much lower than the percentage of the MF.

Finally, we make an additional plot where we represent, for both frequencies, the number of real sources detected vs. the number of the spurious sources (Figure 6). In this way, what we represent is the number of sources that a method detects given a number of spurious sources. If we compare both plots, we can see that the curve of the MMF is always above the MF. It means that, when we have a fixed number of spurious detections, we detect more real sources with the MMF.

We have to point out that the plots that we have introduced here are not directly comparable to Figure 1. As we have seen in this section, there are three basic and important differences:

- A different way to simulate the point sources.
- A different level of detection (in this case, a 3σ level).
- In Figure 1 we represent the number of sources with the corresponding flux in the horizontal axis. In the plots of this section, what we represent is the number of sources whose fluxes are higher than the corresponding value in the horizontal axis.

We can say that this new multifrequency method is better in the sense that the number of detected sources is higher below $\sim 0.4 - 0.5$ Jy and ~ 0.2 at 44 and 100 GHz respectively. And the reliability of the MMF is higher for fluxes below ~ 0.9 Jy and ~ 0.25 Jy at 44 GHz and 100 GHz, respectively.

5 CONCLUSIONS

The detection of extragalactic point sources in CMB maps is a challenge. One has to remove them to do a proper study

of the cosmic radiation. In addition, it is of great interest to study their properties, spatial and spectral distributions, etc. For this reason, we need suitable tools to detect and extract these sources. There are many filtering techniques that have been used in this context. In this work, we have used the matched filter, one of the most studied techniques, and we have compared it with a new multifrequency one based on the matched multifilter (MMF). The great difference is that the latter takes into account information from all the channels of the same sky region in a simultaneous way. In particular, we show an example for $N = 2$.

The different tests that we have used have shown an improvement in the results obtained by the MMF with respect to the traditional matched filter. The number of detections is always higher when the MMF is used. In Figure 1 we see that we have a high number of detections with the MMF, even for small values of I_0 . It should be studied in more detail, but it is easy to see that one could detect and characterize point sources with low fluxes for $\gamma < 0$. For this reason, this tool is a powerful technique to detect faint sources in CMB maps.

Another important aspect is to give a good estimation of the quantities that we have chosen to determine the sources, basically the spectral index and the flux at the reference frequency. In both cases, we can see that the MMF improves the results obtained with the matched filter: the values are close to the input values with smaller error bars (with one exception, the determination of the spectral index for $I_0 \lesssim 0.5$ Jy at positive values of the input γ). This is a significant fact in order to be able to detect and study properly these kind of sources.

Additionally, we have made a set of more realistic simulations in order to study and compare both filters in the sense of the spurious sources. We have also changed the threshold detection from 5σ to 3σ to find more spurious sources and make a more complete statistical analysis. First of all, we compare the number of real detections that we obtain with both techniques at 44 and 100 GHz. Comparing the plots of the Figure 4, we appreciate that, at lower fluxes, we detect more real sources with the matched multifilter than with matched filter. This aspect is more notorious at 44 GHz.

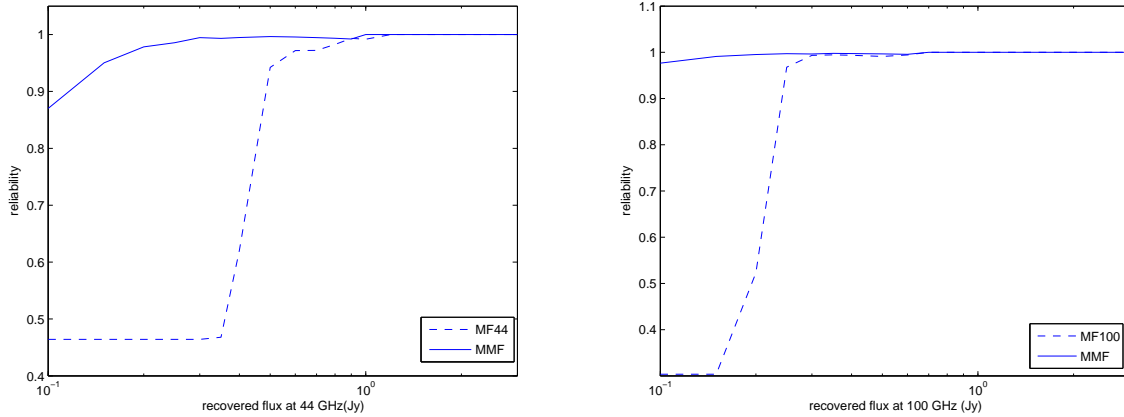


Figure 5. Reliability versus recovered flux for the MMF (solid line) and the MF (dashed line) at 44 GHz (left panel) and 100 GHz (right panel).

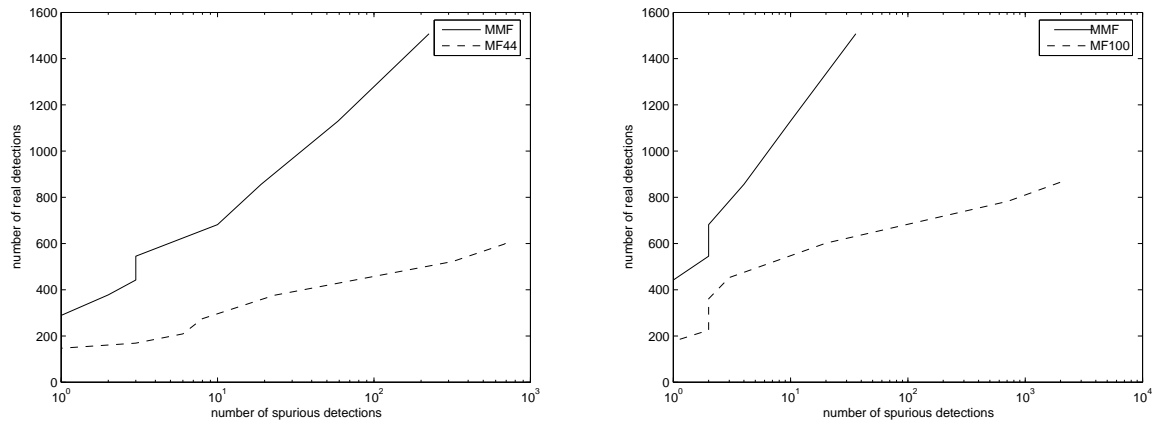


Figure 6. Number of real sources recovered by the MMF (solid line) and the MF (dashed line) at 44 GHz (left panel) and 100 GHz (right panel) vs. the number of spurious sources.

One can also study the reliability of both methods. One can obtain a high number of real detections, and simultaneously find a large number of spurious sources. Precisely, the reliability is a quantity that gives the number of real detections over the total number of sources detected. Comparing the plots of the Figure 5, one can observe that the reliability of the matched multifilter is much higher than the reliability of the matched filter for low fluxes. This difference is particularly important at 44 GHz, where the matched filter obtains similar values to the reliability of the matched multifilter only for fluxes close to 1 Jy. At 100 GHz, the matched filter reaches the reliability of the MMF at 3 Jy.

The last aspect that we use to compare both methods is to look at the number of real sources that we have for a fixed number of spurious detections. The most efficient method is the one that has higher number of real detections for the same value of spurious detections. If we see the Figure 6, the best method is the MMF because its curves are always above the MF. This means that, if we take a number of spurious sources, the MMF recovers a larger number of real objects.

Finally, we have commented at the beginning of the

subsection 2.3 the possibility of devising a filtering method (the MTXF) that does not use the frequency dependence of the sources altogether, totally independent of the frequency behaviour of the sources (flat, steep or inverted). This fact is significant in the sense that this filtering method is a robust technique for changes of f_ν . By contrast, it is necessary to impose the condition of orthonormalisation of the matrix of the filters (see Herranz & Sanz (2008) and Herranz et al. (2009) for more details). This condition minimizes the power of the method. Meanwhile, the MMF is more optimal in the sense of the SNR (see section 2.3), but more complicated because we have to maximize another set of parameters (f_ν). As one can see, the MTXF and the MMF are complementary.

ACKNOWLEDGEMENTS

The authors acknowledge partial financial support from the Spanish Ministry of Education (MEC) under project ESP2004-07067-C03-01 and the joint CNR-CSIC research project 2006-IT-0037. LFL acknowledges the Spanish CSIC

for a JAE-Predoc fellowship and the hospitality of the Osservatorio Astronomico di Padova (INAF) during a research stay. Partial financial support for this research has been provided to JLS by the Spanish MEC and to JG-N by the Italian ASI (contracts Planck LFI Activity of Phase E2 and I/016/07/0 COFIS) and MUR. JG-N also acknowledges a researcher position grant at the SISSA (Trieste). ML-C acknowledges a postdoctoral fellowship from EGEE-III (FP7 INFOS-RI 222667). The authors acknowledge the use of the Planck Sky Model, developed by the Component Separation Working Group (WG2) of the Planck Collaboration.

REFERENCES

- Barreiro R. B., Sanz J. L., Herranz D., Martínez-González E., 2003, *MNRAS*, 342, 119
- Bartlett J. G., Chamballu A., Melin J.-B., Arnaud M., Members of the Planck Working Group 5 2008, *Astronomische Nachrichten*, 329, 147
- Bedini L., Herranz D., Salerno E., Baccigalupi C., Kuruoğlu E. E., Tonazzini A., 2005, *EURASIP Journal on Applied Signal Processing*, 15, 2400
- Bennett C. L., Bay M., Halpern M., Hinshaw G., Jackson C., Jarosik N., Kogut A., Limon M., Meyer S. S., Page L., Spergel D. N., Tucker G. S., Wilkinson D. T., Wollack E., Wright E. L., 2003, *ApJ*, 583, 1
- Bonaldi A., Bedini L., Salerno E., Baccigalupi C., De Zotti G., 2006, *MNRAS*, 373, 271
- Carlstrom J. E., Holder G. P., Reese E. D., 2002, *ARA&A*, 40, 643
- Carvalho P., Rocha G., Hobson M. P., 2009, *MNRAS*, 393, 681
- Chen X., Wright E. L., 2008, *ApJ*, 681, 747
- Chiang L.-Y., Jørgensen H. E., Naselsky I. P., Naselsky P. D., Novikov I. D., Christensen P. R., 2002, *MNRAS*, 335, 1054
- De Zotti G., Ricci R., Mesa D., Silva L., Mazzotta P., Toffolatti L., González-Nuevo J., 2005, *A&A*, 431, 893
- De Zotti G., Toffolatti L., Argüeso F., Davies R. D., Mazzotta P., Partridge R. B., Smoot G. F., Vittorio N., 1999, in Maiani L., Melchiorri F., Vittorio N., eds, *3K cosmology Vol. 476 of American Institute of Physics Conference Series, The Planck Surveyor Mission: Astrophysical Prospects*. pp 204–+
- Delabrouille J., Cardoso J.-F., Patanchon G., 2003, *MNRAS*, 346, 1089
- Delabrouille et al. 2009, in preparation
- Dickinson C., Davies R. D., Davis R. J., 2003, *MNRAS*, 341, 369
- Diego J. M., Vielva P., Martínez-González E., Silk J., Sanz J. L., 2002, *MNRAS*, 336, 1351
- Eddington A. S., 1913, *MNRAS*, 73, 359
- Eriksen H. K., Banday A. J., Górski K. M., Lilje P. B., 2004, *ApJ*, 612, 633
- Finkbeiner D. P., Davis M., Schlegel D. J., 1999, *ApJ*, 524, 867
- González-Nuevo J., Argüeso F., López-Caniego M., Toffolatti L., Sanz J. L., Vielva P., Herranz D., 2006, *MNRAS*, 369, 1603
- González-Nuevo J., Massardi M., Argüeso F., Herranz D., Toffolatti L., Sanz J. L., López-Caniego M., De Zotti G., 2008, *MNRAS*, 384, 711
- González-Nuevo J., Toffolatti L., Argüeso F., 2005, *ApJ*, 621, 1
- Haslam C. G. T., Salter C. J., Stoffel H., Wilson W. E., 1982, *A&AS*, 47, 1
- Herranz D., Gallegos J., Sanz J. L., Martínez-González E., 2002c, *MNRAS*, 334, 533
- Herranz D., López-Caniego M., Sanz J. L., González-Nuevo J., 2009, *MNRAS*, 394, 510
- Herranz D., Sanz J. L., 2008, *IEEE Journal of Selected Topics in Signal Processing*, 5, 727
- Herranz D., Sanz J. L., Barreiro R. B., López-Caniego M., 2005, *MNRAS*, 356, 944
- Herranz D., Sanz J. L., Barreiro R. B., Martínez-González E., 2002b, *ApJ*, 580, 610
- Herranz D., Sanz J. L., Hobson M. P., Barreiro R. B., Diego J. M., Martínez-González E., Lasenby A. N., 2002a, *MNRAS*, 336, 1057
- Hinshaw G., Nolte M. R., Bennett C. L., Bean R., Doré O., Greason M. R., Halpern M., Hill R. S., Jarosik N., Kogut A., Komatsu E., 2007, *ApJS*, 170, 288
- Hobson M. P., Barreiro R. B., Toffolatti L., Lasenby A. N., Sanz J. L., Jones A. W., Bouchet F. R., 1999, *MNRAS*, 306, 232
- Hobson M. P., McLachlan C., 2003, *MNRAS*, 338, 765
- Jiang H., Chen W. R., Liu H., 2002, *IEEE Transactions on Biomedical Engineering*, 11, 1270
- Leach et al. 2008, *A&A*, 491, 597
- López-Caniego M., González-Nuevo J., Herranz D., Massardi M., Sanz J. L., De Zotti G., Toffolatti L., Argüeso F., 2007, *ApJS*, 170, 108
- López-Caniego M., Herranz D., Barreiro R. B., Sanz J. L., 2004, in Bouman C. A., Miller E. L., eds, *Computational Imaging II*. Edited by Bouman, Charles A.; Miller, Eric L. *Proceedings of the SPIE, Volume 5299*, pp. 145–154 (2004). Vol. 5299 of Presented at the Society of Photo-Optical Instrumentation Engineers (SPIE) Conference, A Bayesian approach to filter design: detection of compact sources. pp 145–154
- López-Caniego M., Herranz D., Barreiro R. B., Sanz J. L., 2005, *MNRAS*
- López-Caniego M., Herranz D., González-Nuevo J., Sanz J. L., Barreiro R. B., Vielva P., Argüeso F., Toffolatti L., 2006, *MNRAS*, 370, 2047
- López-Caniego M., Herranz D., Sanz J. L., Barreiro R. B., 2005, *EURASIP Journal on Applied Signal Processing*
- López-Caniego M., Massardi M., González-Nuevo J., Lanz L., Herranz D., De Zotti G., Sanz J. L., Argüeso F., 2009, submitted
- Maino D., Farusi A., Baccigalupi C., Perrotta F., Banday A. J., Bedini L., Burigana C., De Zotti G., Górski K. M., Salerno E., 2002, *MNRAS*, 334, 53
- Massardi M., López-Caniego M., González-Nuevo J., Herranz D., De Zotti G., Sanz J. L., 2009, *MNRAS*, 392, 733
- Melin J.-B., Bartlett J. G., Delabrouille J., 2006, *A&A*, 459, 341
- Naselsky P., Novikov D., Silk J., 2002, *MNRAS*, 335, 550
- Pierpaoli E., Anthoine S., Huffenberger K., Daubechies I., 2005, *MNRAS*, 359, 261
- Pires S., Juin J. B., Yvon D., Moudou Y., Anthoine S.,

- Pierpaoli E., 2006, *A&A*, 455, 741
- Sadler E. M., Ricci R., Ekers R. D., Sault R. J., Jackson C. A., de Zotti G., 2008, *MNRAS*, 385, 1656
- Sanz J. L., Herranz D., López-Cañiego M., Argüeso F., 2006, in *Proceedings of the 14th European Signal Processing Conference (2006)*. EUSIPCO 2006 Conference, Wavelets on the sphere. Application to the detection problem. pp 1–5
- Sanz J. L., Herranz D., Martínez-González E., 2001, *ApJ*, 552, 484
- Schäfer B. M., Pfrommer C., Hell R. M., Bartelmann M., 2006, *MNRAS*, 370, 1713
- Stolyarov V., Hobson M. P., Ashdown M. A. J., Lasenby A. N., 2002, *MNRAS*, 336, 97
- Sunyaev R. A., Zeldovich Y. B., 1970, *Comments on Astrophysics and Space Physics*, 2, 66
- Sunyaev R. A., Zeldovich Y. B., 1972, *Comments on Astrophysics and Space Physics*, 4, 173
- Tauber J. A., 2005, in Lasenby A. N., Wilkinson A., eds, *New Cosmological Data and the Values of the Fundamental Parameters Vol. 201 of IAU Symposium, The Planck Mission*. pp 86–+
- Tegmark M., de Oliveira-Costa A., 1998, *ApJL*, 500, L83+
- The Planck Collaboration 2006, *ArXiv Astrophysics e-prints*
- Toffolatti L., Argüeso Gómez F., De Zotti G., Mazzei P., Franceschini A., Danese L., Burigana C., 1998, *MNRAS*, 297, 117
- Tucci M., Martínez-González E., Toffolatti L., González-Nuevo J., De Zotti G., 2004, *MNRAS*, 349, 1267
- Tucci M., Martínez-González E., Vielva P., Delabrouille J., 2005, *MNRAS*, 360, 935
- Vale C., White M., 2006, *New Astronomy*, 11, 207
- Vielva P., Barreiro R. B., Hobson M. P., Martínez-González E., Lasenby A. N., Sanz J. L., Toffolatti L., 2001, *MNRAS*, 328, 1
- Vielva P., Martínez-González E., Gallegos J. E., Toffolatti L., Sanz J. L., 2003, *MNRAS*, 344, 89
- Wright E. L., Chen X., Odegard N., Bennett C. L., Hill R. S., Hinshaw G., Jarosik N., Komatsu E., Nolte M. R., Page L., Spergel D. N., 2009, *ApJS*, 180, 283